AUTOMATIC SEGMENTATION OF CARDIAC SHORT AXIS SLICES IN PERFUSION MRI

Ganesh Adluru[1, 2], Edward V.R. DiBella[2, 3] and Ross T. Whitaker[4]

[1]Electrical and Computer Engineering, University of Utah
[2] Department of Radiology, University of Utah
[3] Department of Bioengineering, University of Utah
[4] School of Computing, University of Utah

ABSTRACT

Segmentation of the myocardium in dynamic contrast enhanced MR short axis images is an important step towards the estimation of semi-quantitative or quantitative parameters to determine the perfusion to the tissue regions. The perfusion indices of the tissue are obtained by dividing the tissue into regions of interest and estimating perfusion to each region. A fast automatic segmentation method based on level sets has been developed that makes use of the spatial and temporal information available in the dynamic images. The algorithm is validated on cardiac data qualitatively and quantitatively by comparing against regional flow indices from manually segmented tissue regions.

1. INTRODUCTION

Cardiac MR perfusion is a promising tool to detect and characterize coronary artery disease. The contrast agent Gd-DTPA is injected and perfusion images are rapidly acquired using ECG gated sequences to track the uptake and washout of the contrast agent in the heart.

Segmenting the myocardium is an important step in estimating the blood flow to the tissue. The myocardium is divided into regions of interest (ROIs) and a flow estimate for each of the regions is obtained by fitting the mean of the signal intensity time curves in the region to a model [1,2]. To ensure consistency in the regions over the entire perfusion sequence, the myocardium is typically segmented by manually drawing contours on a single reference frame and the same masks for the regions are used on all of the time frames of the registered perfusion sequence. Accurate segmentation of the tissue is required so that there is no region from outside the tissue affecting the flow parameters leading to an incorrect diagnosis. The segmentation is time consuming and in some datasets it is difficult to draw contours because of poor contrast between the myocardium and other regions. Manual segmentation requires expert knowledge and suffers from variability across observers.

A few semi-automatic methods have been proposed towards the segmentation of the myocardium in dynamic perfusion images [3-5]. Much more effort has been directed at segmenting gated wall motion sequences [6-10]. Gated wall motion studies are cine recordings used to image the heart in different phases of the heart cycle with no apparent change in heart contrast. Dynamic perfusion datasets often require more robust methods due to the presence of noise, respiratory motion, changing contrast and poor data quality. Spreeuwers et al. [3] used a region growing method to segment the left ventricle and right ventricle blood pools in perfusion datasets. They segmented the epicardium using a five-node snake on a myocardium feature image. The myocardium feature image was obtained by subtracting maximum intensity projections in the time dimension for two temporal regions. Two fixed nodes of the snake were determined by the segmented right ventricle extrema. This approach gave visually reasonable results, but was not quantitatively evaluated. The method required choosing the temporal regions to get the feature image for the myocardium. Also the method required the presence of the segmented right ventricle blood pool to segment the epicardium. In some apical slices the right ventricle is not present.

Santarelli et al. [4] used a method based on gradient vector flow snakes which required manual tracing of a coarse polygon in the left ventricle to segment the myocardium. Most other methods to date require many parameters to be tuned to get satisfactory results.

The work here improves on our semi-automatic level set based segmentation method in [5] which used both spatial and temporal information. In that approach the final shape of the segmented myocardium was constrained by a-priori determined shape models, as proposed in [11]. The method required the manual selection of a few seeds in the myocardium and choosing a shape model that depended on the slice to be segmented. Here we propose an automatic method which requires no manual interaction and does not use shape models. The new approach uses a level set based framework and the temporal and spatial information in the perfusion images to achieve segmentation of the myocardium.

2. METHODS

2.1 Registration

The dynamic perfusion images were initially registered to a reference image chosen from the temporal center of the sequence to correct for translations in horizontal and vertical directions. Such translations commonly arise due to respiratory motion. Registration was done by minimizing the mean squared difference between the reference frame and all the other perfusion images. A spatial weighting function was used to weight the squared differences. A 2D raised cosine function (Hanning window) was used to penalize the square of the intensity difference more in the center region of the image as compared to outer regions. The registration step was used to make the next step of finding the location of the heart more robust.

2.2 Finding the heart

In the perfusion images the changing contrast in the left ventricular and right ventricular blood pools creates high temporal variance in the blood pools. A variance image was generated by computing the variance of temporal pixel intensities. In order to reduce the effects due to residual respiratory motion of the heart and other structures in the images, the variance image was generated using only a few image frames in the temporal sequence. The frames used to compute the variance image were chosen based on the sum of all the pixel intensities for each frame. The sum for each image in the temporal sequence gradually increases as the contrast agent enters the right ventricle blood pool and reaches the left ventricle blood pool. The starting frame used to compute the variance was chosen after the point where the sum follows an increasing pattern in three consecutive frames to reduce the variance of right ventricle blood pool. The end frame to compute the variance was chosen such that the contrast agent was in the tissue. The end frame was chosen 17 frames after the starting frame.

After finding the starting and the ending time frames to be used to compute the variance image, the images in the range were smoothed to reduce the noise. The variance image was computed using the smoothed images and the 2D raised cosine spatial weighting function was applied on the variance image to weight more the left ventricle blood pool. A seed in the left ventricle blood pool was determined as the location of the maximum value in the weighted variance image. Figure 1a shows the weighted variance image for a typical dataset.

2.3 Segmenting the myocardium

Figure 1b shows the seed in the left ventricle blood pool obtained by finding the maximum value in the weighted variance image in Figure 1a. A reference image was chosen at the peak of the signal intensity time curve of the seed pixel. Using the seed index a polar map was generated by going radially outward from the seed in the left ventricle blood pool in the reference image. Figure 1c shows the polar map from the seed shown in Figure 1b. The endocardium in the polar map was segmented using intensity thresholding (a lower threshold fraction of 0.6 of the intensity of the seed found in left ventricle was used) due to the good contrast between the left ventricle blood pool and the endocardium. Seeds in the myocardium were then found by going outward three pixels from the segmented left ventricle blood pool in the polar map. The polar map was only used to get the seeds in the myocardium. The seed indices were converted back into Cartesian space and input to a level set based framework. The implementation was based on routines available in ITK [12].

Level sets have been widely used in the segmentation of medical images. In this approach a curve is implicitly represented as a zero level set of a higher dimensional function ϕ and the entire function is evolved according to a differential equation. The terms in the differential equation are used to constrain the evolution of the function ϕ. Most of the terms in the equation are based on the spatial features of the image to be segmented although in our previous work [5], we incorporated temporal information in the evolution equation by using a spectral speed function as proposed in [13] that accounts for the selected images in the perfusion sequence. The embedded curve deforms as ϕ evolves and segments the object of interest.

In the current implementation, the differential equation governing the evolution of the function is given by

$$\frac{\partial(\phi)}{\partial t} = -\lambda_1 P(\mathbf{x})\left|\nabla(\phi)\right| + \lambda_2 \kappa \left|\nabla(\phi)\right| \quad \text{- (1)}$$

In the above equation P is the intensity based propagation term, κ is the curvature term for smoothness of the evolving surface and controls leaking into other structures. λ_1 and λ_2 are the weighting factors for the propagation and curvature terms respectively. The propagation term P is calculated from the input image g with upper threshold U and lower threshold L according to

$$P(\mathbf{x}) = \begin{cases} g(\mathbf{x}) - L; \ if \ \ g(\mathbf{x}) < (U-L)/2 + L \\ U - g(\mathbf{x}); \ otherwise \end{cases} \quad \text{- (2)}$$

The function is evolved iteratively and the binary image of segmented object is obtained by performing a binary thresholding on the output function obtained after the iterations. The upper and lower thresholds required in the above equation to segment the myocardium were determined as fractions (1.4 and 0.6 respectively) of the median of the intensities of the seeds found in the tissue. The parameters λ_1 and λ_2 were chosen as 1 and 25 respectively. The level sets were evolved until the root-mean-square change in the level set function was below 0.02 or the number of iterations reached 1200. The binary mask of segmented myocardium was obtained after the evolution of ϕ.

2.4 Use of adjacent frames

In some datasets a single reference frame chosen as above was not sufficient to get accurate segmentation of the myocardium due to poor contrast between the tissue and other regions. We make use of the fact that there is more than one frame with different contrast between the myocardium and the blood pools when the contrast agent uptake is in the tissue. We repeated the above method of segmenting the myocardium on the two image frames before and the two image frames chosen after the initial reference frame. The segmented myocardial masks were then registered using the mean squared difference method to correct for any residual motion and a mask, which was the sum of the five masks, was obtained. The final segmented myocardial mask was obtained by binary thresholding (a threshold factor of four was used) the sum mask. This was helpful to remove any leaking if present in some frames. Figure 1d shows the final result of segmentation for the typical dataset.

3. TEST DATASETS

The algorithm was tested on 16 short axis datasets from eight different patients, two slices each. Five patients and one volunteer were imaged with a saturation recovery turboFLASH sequence on a Siemens Trio 3T. One patient and one volunteer were imaged with a fast gradient echo train sequence on a GE Signa 1.5T scanner. Seven of the 16 datasets were adenosine stress perfusion data and nine were rest perfusion data. Reconstructed pixel size varied between 1.7 mm and 1.9 mm. The results of the segmented myocardium were assessed visually and by performing two-

compartmental model [1] analysis of the segmented tissue. The myocardium was divided into eight ROIs as shown in Figure 2 and the mean flow indices for each ROI were obtained. Manual segmentation was performed by a trained user. The flow indices obtained using the manual segmentation were compared with those obtained using the automatic method.

4. RESULTS

The results of the automatically segmented myocardium matched well with the edges of the myocardium in the datasets. Figure 3 shows one frame of automatically segmented myocardium in four datasets. The flow indices for the eight regions obtained using manual segmentation and the fully automatic method for the dataset in Figure 1d are given in table 1. The average relative error in the flow indices for the eight regions is 0.07. Paired t-tests were performed between the flow indices of the ROIs obtained with the manual segmentation and the automatic method at significance level of $P<0.05$ for the 128 regions in 16 datasets. The flow indices were not significantly different ($P=0.492$).

5. DISCUSSION

An automatic segmentation method for cardiac perfusion short axis slices was presented. For all of the datasets tested using this algorithm, no parameters of the segmentation algorithm were changed. Although registration was an important step to determine the location of the heart, a coarse registration was sufficient. In some cases, if the subject had a good breath-hold, no registration was required. The smoothing of the frames used to calculate the variance image helped to reduce the outliers in the variance image caused due to change of shape of structures in the liver in a few datasets.

In our previous work we incorporated shape information in the segmentation of myocardium in which deformable shape models for a basal slice, mid slice and apical slices were created. Each 2D shape model was trained for a particular axial slice. The results in this paper show that the shape model may not be necessary if we use a sufficiently high weighting for the curvature term in equation (1) and more than one frame from the dynamic sequence to segment the myocardium. Figure 4 shows an example dataset in which there was leaking of the segmented myocardium into the right ventricle in one frame due to the poor contrast. But the leaking was prevented in the final segmented myocardium by using adjacent time frames in which the contrast of the myocardium was different from that in the right ventricle. Also the high weighting on the curvature term prevented leakage of level sets into papillary muscles.

6. CONCLUSION

A method for segmenting the left ventricular myocardium in short axis slices from dynamic contrast enhanced MRI datasets was developed and tested. Clinically useful flow index parameters of the tissue regions obtained from the automatic segmentation matched well with those obtained from manual segmentation. The time taken by the algorithm to segment a typical dataset on a Pentium IV 2.2 GHz processor with 256 MB of RAM was 16 seconds. The results show that using spatial and temporal information as in this method achieves robust results efficiently.

Acknowledgements: This work was supported by NIH R01 EB000177. The authors thank Nathan Pack for performing manual segmentation of the datasets.

7. FIGURES AND TABLES

Figure 1

(a) (b) (c) (d)

(a) Weighted variance image computed from the dynamic dataset of a typical patient
(b) Seed found in the left ventricular blood pool using the maximum value in the variance image shown in Figure 1a
(c) Polar map generated by going radially outward from the seed found in Figure 1b (X = radius, Y = angle)
(d) A single time frame of the final segmented myocardium obtained using the level set based framework is shown

Figure 2

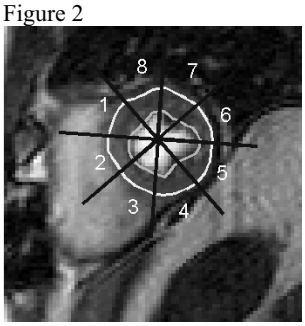

Division of the manually segmented myocardium into eight regions to estimate the flow indices for each region

Table 1

Region	Flow index for manually segmented tissue	Flow index for automatically segmented tissue
1	1.2522	1.2514
2	1.0426	0.7808
3	1.1216	0.9020
4	1.0448	1.0484
5	0.9490	1.0072
6	0.7806	0.7896
7	1.1846	1.1394
8	1.3601	1.3364

Comparison of the manually and automatically segmented flow indices of each region of the perfusion dataset shown in Figure 1

Figure 3

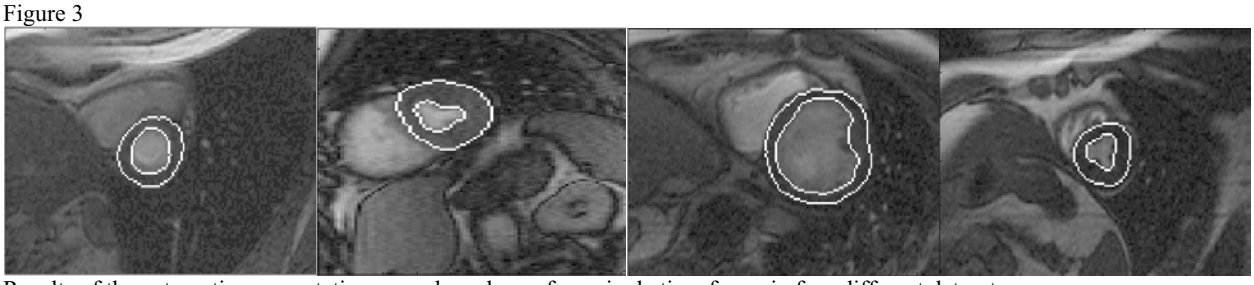

Results of the automatic segmentation procedure shown for a single time frame in four different datasets

Figure 4

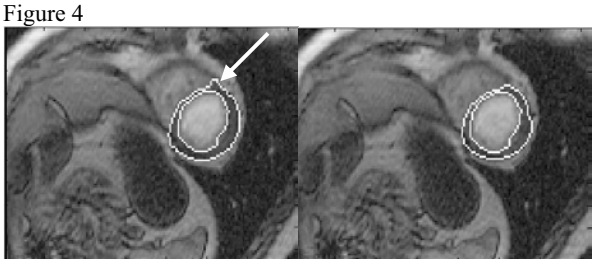

(a) (b)

(a) – Segmentation of myocardium using a single time frame in which there is 'leakage' at the arrow shown
(b) – Segmentation of myocardium using five time frames resolving the leakage

11. REFERENCES

[1] J.P. Vallee, F. Lazeyras, L. Kasuboski, P. Chatelain, N. Howarth, A. Righetti, D. Didier, "Quantification of myocardial perfusion with FAST sequence and Gd bolus in patients with normal cardiac function," *J Magn Reson Imaging*, Vol 9(2), pp.197-203, 1999

[2] T.F. Christian, D.W. Rettmann, A.H. Aletras, S.L. Liao, J.L. Taylor, R.S. Balaban, A.E. Arai, "Absolute Myocardial Perfusion in Canines Measured by Using Dual-Bolus First-Pass MR Imaging," *Radiol.*, Vol. 232, pp.677-684, 2004

[3] L. Spreeuwers and M. Breeuwer, "Automatic Detection of Myocardial Boundaries in MR Cardio Perfusion Images," *MICCAI 2001,* LNCS 2208, pp. 1228-1231, 2001

[4] M.F. Santarelli, V. Positano, C. Michelassi, M. Lombardi, L. Landini, "Automated cardiac MR image segmentation: theory and measurement evaluation," *Med. Eng. Phys.,* Vol 25(2), pp.149-159, 2003

[5] L. Lorenzo, R.S. MacLeod, R.T. Whitaker, G. Adluru, E.V.R. DiBella, "Level sets and shape models for segmentation of cardiac perfusion MRI," To appear in *SPIE Medical Imaging Conference,* 2006

[6] D.T. Gering, "Automatic Segmentation of Cardiac MRI," *MICCAI 2003*, LNCS 2878, pp. 524-532, 2003

[7] M.R. Kaus, J.V. Berg, J. Weese, W. Niessen and V. Pekar, "Automated segmentation of the left ventricle in cardiac MRI," *Med. Image Anal.,* Vol 8(3), pp. 245-254, 2004

[8] S. Julien, C.A. Chris, N Thomas, "Model-based segmentation of cardiac MRI cine sequences: a Bayesian formulation," *Proc. SPIE Medical Imaging Conference,* Vol 5370, pp.432-443, 2004

[9] M.P. Jolly, N Duta, G. Funka-Lea, "Segmentation of the left ventricle in cardiac MR images," *Proc. IEEE ICCV,* Vol 1, pp.773-776, 2001

[10] I. Shin, M.J. Kwon, S.T. Chung, H.W. Park, "Segmentation and visualization of left ventricle in MR cardiac images," *Proc. IEEE ICIP,* Vol 2, pp. II-89 – II-92, 2002

[11] M.E. Leventon, W.E.L. Grimson, O.Faugeras, "Statistical shape influence in geodesic active contours," *Proc. IEEE CVPR,* Vol 1, pp.316-323, 2000

[12] T. S. Yoo, M.J. Ackerman, W.E. Lorensen, W. Schroeder, V. Chalana, S. Aylward, D. Metaxas, R.T. Whitaker, "Engineering and Algorithm Design for an Image Processing API: A Technical Report on ITK - the Insight Toolkit", *Studies in Health Technology and Informatics,* Vol. 85, Amsterdam: IOS Press, pp. 586-592, 2002

[13] J. Cates, A. Lefohn, R.T. Whitaker, Gist: An interactive, gpu-based level set segmentation tool for 3d medical images," *Med. Image Anal.,* Vol. 8, Issue 3, pp. 217-231, 2004